

Papers published in *Hydrology and Earth System Sciences Discussions* are under open-access review for the journal *Hydrology and Earth System Sciences*

# A conceptual model of flow to the Waikoropupu Springs, NW Nelson, New Zealand, based on hydrometric and tracer ( $^{18}\text{O}$ , $\text{Cl}$ , $^3\text{H}$ and CFC) evidence

M. K. Stewart<sup>1,\*</sup> and J. T. Thomas<sup>2</sup>

<sup>1</sup>GNS Science, Lower Hutt, New Zealand

<sup>2</sup>Tasman District Council, Richmond, New Zealand

\* now at: Aquifer Dynamics Ltd, Lower Hutt, New Zealand

Received: 27 April 2007 – Accepted: 13 May 2007 – Published: 31 May 2007

Correspondence to: M. K. Stewart (mk.stewart@gns.cri.nz)

**HESSD**

4, 1215–1264, 2007

## Conceptual flow model for karst springs

M. K. Stewart and  
J. T. Thomas

Title Page

Abstract

Introduction

Conclusions

References

Tables

Figures

⏪

⏩

◀

▶

Back

Close

Full Screen / Esc

Printer-friendly Version

Interactive Discussion

## Abstract

The Waikoropupu Springs, a large karst resurgence 4 km from the coast, are supplied by the Arthur Marble Aquifer (AMA) underlying the Takaka Valley, South Island, New Zealand. New evidence on the recharge sources in the catchment, combined with previous results, is used to establish a new recharge model for the AMA. Combined with the oxygen-18 mass balance, this yields a quantitative description of the inputs and outputs to the aquifer. It shows that the Main Spring is sourced mainly from the karst uplands (74%), with smaller contributions from the Upper Takaka River (18%) and valley rainfall (8%), while Fish Creek Spring contains mostly Upper Takaka River water (50%). In addition, much of the Upper Takaka River contribution to the aquifer (58%) bypasses the springs and is discharged offshore via submarine springs. The chemical concentrations of the Main Spring show input of 0.5% of sea water on average, which varies with flow and derives from the deep aquifer. Tritium measurements spanning 40 years, and CFC-11 measurements, give a mean residence time of 8 years for the Main Spring water using the preferred two-component model. Our conceptual flow model, based on the flow, chloride, oxygen-18 and age measurements, invokes two different flow systems with different recharge sources to explain the flow within the AMA. One system contains deeply penetrating old water with mean age 10.2 years and water volume 3 km<sup>3</sup>, recharged from the karst uplands. The other, at shallow levels below the valley floor, has much younger water, with mean age 1.2 years and water volume 0.4 km<sup>3</sup>, recharged by Upper Takaka River and valley rainfall. The flow systems contribute in different proportions to the Main Spring, Fish Creek Springs and offshore springs. Their very different behaviours, despite being in the same aquifer, are attributed to the presence of a diorite intrusive below the surface of the lower valley, which diverts the deep flow towards the Waikoropupu Springs and allows much of the shallow flow to pass over the intrusive and escape via submarine springs.

HESSD

4, 1215–1264, 2007

### Conceptual flow model for karst springs

M. K. Stewart and  
J. T. Thomas

Title Page

Abstract

Introduction

Conclusions

References

Tables

Figures

◀

▶

◀

▶

Back

Close

Full Screen / Esc

Printer-friendly Version

Interactive Discussion

# 1 Introduction

The Arthur Marble Aquifer (AMA) underlies the Takaka Valley on the South Island of New Zealand (Figs. 1, 2), and supplies the Waikoropupu Springs comprising the Main Spring, Dancing Sands Spring and Fish Creek Springs (Fig. 3). Waikoropupu Springs are locally known as Pupu Springs and both terms are used in this paper for the collective discharges. The springs are New Zealand's largest and an impressive sight; their average flow is 13 300 l/s. They are karstic, tidal and slightly brackish. The springs emerge from Arthur Marble through a cover of Motupipi Coal Measures approximately 4 km south of Golden Bay and 14–17 m above sea level. The source of the water has been at issue since the end of the last century (Park, 1890).

The mystique of the springs has to do with their size, clarity and attractive setting, but the springs have many interesting features. Their sheer size suggests that they are drawn from a diversity of sources over a wide area in company with large karstic springs elsewhere in the world (Ford and Williams 1989; Williams, 2004). The Pupu Springs are the main discharge zone of the AMA. Arthur Marble also outcrops east and west of the lower valley, and in the upper headwaters of the Waitui Stream (Fig. 2). Several investigations in the late 1970s established physical, hydrological, and chemical features of the springs (Michaelis, 1976; Williams, 1977; Stewart and Williams, 1981; Stewart and Downes, 1981). Further work has been reported in the 1980s and 1990s (Mueller, 1987, 1992; Edgar, 1998; Thomas, 2000; Taylor, 2001).

The Pupu Springs lie on the western side of the Takaka Valley (Fig. 1). Williams (1977) demonstrated hydraulic connection between Takaka River water sinking into its bed 16–18 km inland of the springs and the springs themselves by pulse-train analysis, using pulses in the Takaka River flow caused by releases from the upstream Cobb Reservoir. He also discussed the location of the springs and the nature of the subterranean system.

This paper brings together new and existing evidence to improve our understanding of flow in the AMA, and in particular the sources of the Waikoropupu Springs. Hydro-

## Conceptual flow model for karst springs

M. K. Stewart and  
J. T. Thomas

Title Page

Abstract

Introduction

Conclusions

References

Tables

Figures

⏪

⏩

◀

▶

Back

Close

Full Screen / Esc

Printer-friendly Version

Interactive Discussion

metric information on the sources of recharge is critically evaluated and combined with the oxygen-18 mass balance to produce a quantitative recharge/discharge flow model for the AMA. Chloride concentrations of the Main Spring combined with oxygen-18 values point to a two-component flow system. Tritium, CFC and oxygen-18 measurements are used to determine water residence times. Because the tritium measurements on the Main Spring almost cover the rise and fall of tritium in the atmosphere due to nuclear weapons testing in the 1950s and 1960s, they are particularly reliable for determining the mean residence time and the shape of the age distribution.

The various types of evidence are put together to support a conceptual model of flow in the AMA involving two apparently almost independent flow systems. These combine in different proportions to produce the various outflows of the Pupu Springs, and offshore springs.

## 2 Hydrogeological setting

The Takaka River has a catchment area of 928 km<sup>2</sup>, and includes subcatchments of the Waingaro, Anatoki, Waikoropupu Rivers on the west (Fig. 1). Precipitation ranges from 1900–5000 mm/yr between the lowest and highest altitudes. The Anatoki catchment (5000 mm/yr) receives more precipitation per unit area than the Waingaro catchment (3200 mm/yr), which in turn receives more than the Upper Takaka catchment (2700 mm/yr). The decrease in precipitation from west to east is due to the westerly-dominated weather systems, which shed more rainfall on the first mountain ranges they encounter. Mountain range and peak altitudes are about the same in all three sub-catchments.

There are three main water-bearing geological units in the area; 1) the Arthur Marble Aquifer, 2) the Takaka Limestone Aquifer, and 3) the Takaka Valley Unconfined Gravel Aquifer. The hydrologic characteristics of these aquifers are directly related to the lithology/geology of the aquifers.

## Conceptual flow model for karst springs

M. K. Stewart and  
J. T. Thomas

Title Page

Abstract

Introduction

Conclusions

References

Tables

Figures

⏪

⏩

◀

▶

Back

Close

Full Screen / Esc

Printer-friendly Version

Interactive Discussion

## 2.1 Arthur Marble Aquifer

The Arthur Marble Aquifer is the principal karstic aquifer in the Takaka Valley area, and is an aquifer in Ordovician Arthur Marble. Arthur Marble is found underneath the Takaka Valley floor, from Upper Takaka to the Golden Bay coast, and in the mountain ranges parallel to this valley section (Fig. 1). Figure 2 shows northwest-southeast cross-sections (Sections A and B). Marble covers an area of about 180 km<sup>2</sup> in the Central and Lower Takaka subcatchments.

Under the Central Takaka Valley floor the marble is covered by tens of metres of alluvial gravel (45 km<sup>2</sup>) and in the Lower Takaka catchment it is additionally covered by Tertiary formations (45 km<sup>2</sup>) composed of Motupipi Coal Measures, Takaka Limestone and Tarakohe Mudstone.

The Arthur Marble Aquifer is unconfined from Upper Takaka to about Hamama (Fig. 4a). In the unconfined area, Arthur Marble is overlain by cavernous Takaka Limestone and/or permeable alluvial gravels. The aquifer surface is defined by the water table, and the lithological boundary between marble and limestone has no distinguishable influence on groundwater flows. North of Hamama, impervious Motupipi Coal Measures overlie the Arthur Marble and the aquifer surface is defined by the elevation of the base of the Motupipi Coal Measures (Fig. 4a).

The thickness of the marble is up to 1000 m. Dissolution of the marble has caused the formation of a significant surface karstic landscape, with features such as karren, dolines, swallow holes, a strong serrated relief, and a significant subterranean aquifer system. The depth of karstification below the valley is unknown, but given sea level change (to -130 m at the height of the last glaciation 17 000 yr ago) karstification to 1–200 m depth at least would be expected (Ford and Williams, 1989; Fleury et al., 2007).

## Conceptual flow model for karst springs

M. K. Stewart and  
J. T. Thomas

Title Page

Abstract

Introduction

Conclusions

References

Tables

Figures

⏪

⏩

◀

▶

Back

Close

Full Screen / Esc

Printer-friendly Version

Interactive Discussion

## 2.2 Takaka Limestone Aquifer

The Takaka Limestone Aquifer occurs between East Takaka and Tarohe (Fig. 4b) and is a result of karstification processes on Oligocene Limestone. In the northern half of the Valley (north of Hamama and East Takaka), the Takaka Limestone Aquifer is underlain by the Motupipi Coal Measures, which act as an aquiclude. The aquiclude is absent south of Hamama and East Takaka, and the Arthur Marble and Takaka Limestone aquifers are indistinguishable. Takaka Limestone is gently folded into a series of low amplitude synclines and anticlines. Only small amounts of groundwater are abstracted from this aquifer and the aquifer thickness varies between 30 and 60 m.

Recharge to the aquifer is from rainfall, seepage from creeks draining the eastern boundary and inflow from the Upper Takaka River.

## 2.3 Takaka Valley unconfined gravel Aquifer

Quaternary gravel and sand deposits cover most of the Takaka Valley from Upper Takaka to the sea (Fig. 4c). The major water-bearing gravels are the ones underlying the lowest river terraces of the Takaka Valley and Takaka Township. The thickness of the gravels varies down the valley. Around Lindsay's Bridge the gravels are about 10 m thick, whilst recent drilling upstream of East Takaka revealed a gravel thickness of 57 m. The gravel is generally between 5–12 m thick in East Takaka. In the central part of Takaka Township, the gravels are estimated to be 30–40 m thick.

## 3 Sampling and methods

### 3.1 Chemical data

Water samples from rivers, springs, and groundwater wells have been collected by Tasman District Council hydrologists over a number of years. Groundwater wells were purged of at least three casing volumes before samples were taken, following methods

## Conceptual flow model for karst springs

M. K. Stewart and  
J. T. Thomas

Title Page

Abstract

Introduction

Conclusions

References

Tables

Figures

◀

▶

◀

▶

Back

Close

Full Screen / Esc

Printer-friendly Version

Interactive Discussion

outlined in Rosen et al. (1999). Samples for cation analyses were field filtered and acidified with high-purity nitric acid. Anion samples were field filtered and kept below 4°C until analysed and bicarbonate samples were collected unfiltered, kept below 4°C, and analysed within 48 h of collection. Analytical methods have changed for some parameters, but in general the same methods have been used for each collection period. Methods for cation analyses include Atomic Adsorption and ICP-OES, and for anion analyses include auto titrator, auto analyser, and ion chromatography.

### 3.2 Isotopic data

Groundwater bores were purged of at least three casing volumes before samples were taken. Bottles were flushed with the water to be sampled, emptied, refilled with water and allowed to overflow. Care was taken to seal the bottles tightly to prevent evaporation. Samples of water were collected in 28 mL glass bottles for  $^{18}\text{O}$ , and 1.1 L bottles for tritium.

For  $^{18}\text{O}$  measurement, 2 mL of the water is isotopically equilibrated with  $\text{CO}_2$  gas at 29°C for two hours, and then the  $\text{CO}_2$  is analysed in a stable isotope mass spectrometer (Hulston et al., 1981). Oxygen-18 concentrations are expressed as  $\delta^{18}\text{O}$  values, where

$$\delta^{18}\text{O} \text{ in } \text{‰} = \left[ \left( \frac{^{18}\text{O}}{^{16}\text{O}} \right)_{\text{sample}} / \left( \frac{^{18}\text{O}}{^{16}\text{O}} \right)_{\text{VSMOW}} - 1 \right] \times 1000 \quad (1)$$

and VSMOW (Vienna standard mean ocean water) is the standard water. The measurement error is  $\pm 0.1\text{‰}$  (standard error based on analysis of duplicate samples). Oxygen-18 concentrations in water are not affected by interaction with rock at ambient temperature, and therefore are ideal for identifying recharge sources provided there is sufficient contrast in the oxygen-18 concentrations of the possible source waters.

For tritium measurement, samples are distilled, enriched in tritium by a factor of 70 by electrolysis and then counted in a Quantulus low background liquid scintillation counter for several weeks (Taylor, 1994; Morgenstern and Taylor, 2005). Measurement precision was greatly improved in the 1980s and 1990s by methods which have been extensively documented (Taylor, 1994; IAEA, 1995; Morgenstern and Taylor, 2005).

## Conceptual flow model for karst springs

M. K. Stewart and  
J. T. Thomas

Title Page

Abstract

Introduction

Conclusions

References

Tables

Figures

⏪

⏩

◀

▶

Back

Close

Full Screen / Esc

Printer-friendly Version

Interactive Discussion

Measurement errors ( $1\sigma$ ) on samples at the current ambient tritium level are  $\pm 2.8\%$  (about  $\pm 0.04$  TU).

### 3.3 Chlorofluorocarbons

Water samples for CFC concentration measurements were collected in such a way as to prevent contact of the sample with the atmosphere or with plastic materials, either of which could contaminate the water with excess CFCs. The samples were preserved in the field by sealing them into 62 mL borosilicate glass ampoules at the spring or bore site, using methods developed by Busenberg and Plummer (1992) and taught to Vanessa Fox (GNS Science), when she visited the USGS at Reston, VA, USA. Where possible, the sampling apparatus was connected to the bore outlet by copper tubing. All other tubing in contact with the water during sampling was stainless steel. The ampoule was attached to the sampling apparatus and flushed with ultra-high-purity nitrogen gas. The well water was then allowed to flow through the tubing and valves and into the bottom of the ampoule, displacing the nitrogen. The ampoule was rinsed with several hundred millilitres of water, then nitrogen was forced into the neck to displace some of the water. The ampoule was then fused shut about 1–2 cm above the water level with an oxy/acetylene gas torch. Nitrogen flowed continually across the union to prevent any air contamination. Four ampoules were normally collected at each sampling site. The CFC samples were analysed by gas chromatography using an ECD detector.

### 3.4 Residence time determination

The different flow paths of water through the groundwater system means that outflows contain water with a variety of residence times. This distribution of ages is described by a conceptual flow or mixing model, which reflects the average conditions of flow in the system.

Rainfall incident on a catchment can be affected by surface/near surface runoff and evapotranspiration losses. The remainder constitutes recharge to the subsurface wa-

## Conceptual flow model for karst springs

M. K. Stewart and  
J. T. Thomas

Title Page

Abstract

Introduction

Conclusions

References

Tables

Figures

⏪

⏩

◀

▶

Back

Close

Full Screen / Esc

Printer-friendly Version

Interactive Discussion



ter stores; the effects of the recharge processes are considered below. The tracer inputs (tritium and CFC concentrations, temporal  $^{18}\text{O}$  variations in the recharge water) are modified by passing through the hydrological system (as represented by the flow model) before appearing in the output. The convolution integral and an appropriate flow model are used to relate the tracer input and output. The convolution integral is given by

$$C_{\text{out}}(t) = \int_0^{\infty} C_{\text{in}}(t - \tau) h(\tau) \exp(-\lambda\tau) d\tau \quad (2)$$

where  $C_{\text{in}}$  and  $C_{\text{out}}$  are the input and output concentrations in the recharge and outflow respectively.  $t$  is calendar time and the integration is carried out over the transit times  $\tau$ .  $h(\tau)$  is the flow model or response function of the hydrological system. The exponential term accounts for radioactive decay of tritium ( $\lambda$  is the tritium decay constant ( $=\ln 2/T_{1/2}$ , where  $T_{1/2}$  is the half-life of tritium (12.32 years)).

Two flow models are commonly used in tracer studies. The exponential-piston flow model (EPM) combines a volume with exponential transit times followed by a piston flow volume to give a model with two parameters (Maloszewski and Zuber, 1982). The response function is given by

$$h(\tau) = 0 \text{ for } \tau < \tau_m(1 - f) \quad (3a)$$

$$h(\tau) = (f\tau_m)^{-1} \cdot \exp[-(\tau/f\tau_m) + (1/f) - 1] \text{ for } \tau \geq \tau_m(1 - f) \quad (3b)$$

where  $\tau_m$  is the mean residence time, and  $f$  the ratio of the exponential volume to the total volume (Maloszewski and Zuber, 1982, used the parameter  $\eta$ ;  $f=1/\eta$ ).

The dispersion model (DM) assumes a tracer transport which is controlled by advection and dispersion processes (Maloszewski and Zuber, 1982),

$$h(\tau) = \frac{1}{\tau \sqrt{4\pi(D/vx)\tau/\tau_m}} \exp \left[ -\frac{(1 - \tau/\tau_m)^2}{4(D/vx)\tau/\tau_m} \right] \quad (4)$$

**Conceptual flow model for karst springs**

M. K. Stewart and  
J. T. Thomas

Title Page

Abstract

Introduction

Conclusions

References

Tables

Figures

◀

▶

◀

▶

Back

Close

Full Screen / Esc

Printer-friendly Version

Interactive Discussion

where  $D$  is the longitudinal dispersion coefficient,  $v$  is the flow velocity and  $x$  is the flow distance. The parameters are  $\tau_m$  and dispersion parameter ( $DP=D/vx$ ).

Models can be combined to represent more complicated systems, as illustrated by the EPM model above. Based on the understanding of the system gained from the flow,  $^{18}\text{O}$ , chemical and age dating measurements, we have used a model comprising two DM models in parallel; a “double dispersion” model (DDM). The two DMs describe short-residence-time (shallow) and long-residence-time (deep) flow components or systems. The DDM model is simply formed by adding the two DM models:

$$\text{DDM} = b\text{DM}_1 + (1-b)\text{DM}_2 \quad (5)$$

where  $b$  is the fraction of the young component (shallow system fraction). The model has five parameters.

Karst aquifers have special qualities, in particular they are often described as dual porosity media with primary matrix porosity and secondary porosity from solution channels (Ford and Williams, 1989). Maloszewski et al. (2002) noted that in such systems it is not possible to determine the mean transit time of water, but instead the mean transit time of tracer is determined, and that the DM model is the most suitable. Marble is recrystallised limestone, hence the primary porosity will have been reduced during metamorphism, and the aquifer may approximate a channel network alone.

## 4 Results

### 4.1 Recharge sources to the Arthur Marble Aquifer

Recharge to the Arthur Marble Aquifer can occur where Arthur Marble crops out at the surface or is covered by permeable rock such as Takaka Limestone or Quaternary gravels. Possible recharge sources are diverse and include drainage from rivers into sinks as concentrated point or linear inputs and infiltration of precipitation on karst or permeable cover as diffuse inputs.

## Conceptual flow model for karst springs

M. K. Stewart and  
J. T. Thomas

Title Page

Abstract

Introduction

Conclusions

References

Tables

Figures

◀

▶

◀

▶

Back

Close

Full Screen / Esc

Printer-friendly Version

Interactive Discussion

Three groups of recharge sources have been identified as follows:

- Karst uplands on east and west of the valley (fed by sinks in tributary streams in Central Takaka, including the Waingaro and Anatoki Rivers, and rainfall)
- Upper Takaka River sinks
- 5 – Valley rainfall on the Central Takaka Valley

Mueller (1992) considered essentially the same groups of sources, except he separated the Waingaro and Anatoki Rivers from the karst uplands. Edgar (1998) added a fifth source being inter-aquifer leakage from the Takaka Limestone Aquifer, but did not estimate the amount of water being contributed from this source. We consider any  
10 such leakage to be included as part of the rainfall on the Central Takaka Valley.

Recharge from sinking streams in the karst uplands is an important source of water to the underlying aquifers. Fifteen named creeks and other unnamed subcatchments in the Central Takaka Valley (Figs. 1, 4a) generally run dry in their lower reaches. They drain an area of about 170 km<sup>2</sup>. Average precipitation is about 2600 mm/year, with evapotranspiration of 700 mm/year, giving net precipitation of 1900 mm/yr (Mueller, 1992). The uppermost parts of the subcatchments are on impervious bedrock (granite, schist) and flows are on the surface. The creeks then cross onto marble and the flows disappear through the gravel creek beds into cavernous marble. Most of the flows from tributary catchments recharge the Arthur Marble Aquifer and only peak flows reach the  
20 Takaka River. Mueller (1992) estimated that 80% of the total flow in the karst uplands recharges the Arthur Marble Aquifer contributing 8200 l/s on average. Edgar (1998, Sect. 3) estimated that recharge was 50% from a 100 km<sup>2</sup> area yielding their minimum estimate of 3000 l/s recharge. (They excluded the west bank tributaries.) We estimate recharge is 7200 l/s (based on recharge of 70% on 170 km<sup>2</sup>).

25 The Waingaro and Anatoki Rivers cross marble in their middle reaches. Mueller (1992) estimated the loss from the Waingaro River to be 2000 l/s. Edgar's (1998, Sect. 3) estimate was 1,500 l/s. Our estimate is 2000 l/s. (All workers have considered the contribution from Anatoki River to be insignificant.)

---

**Conceptual flow  
model for karst  
springs**

M. K. Stewart and  
J. T. Thomas

---

Title Page

Abstract

Introduction

Conclusions

References

Tables

Figures

⏪

⏩

◀

▶

Back

Close

Full Screen / Esc

Printer-friendly Version

Interactive Discussion

**Conceptual flow model for karst springs**

M. K. Stewart and  
J. T. Thomas

Title Page

Abstract

Introduction

Conclusions

References

Tables

Figures

⏪

⏩

◀

▶

Back

Close

Full Screen / Esc

Printer-friendly Version

Interactive Discussion

The Takaka River commonly runs dry in its reach below Lindsays Bridge (on about 100 days per year, Mueller, 1992) and is an obvious source of recharge to the Arthur Marble Aquifer, as well as to the overlying limestone and gravel aquifers in contact with the AMA (see place names in Fig. 4a). Most of the Takaka Valley from Upper Takaka to the sea is covered with a layer of river gravels. Underneath the gravel, Arthur Marble extends to a depth of several hundred metres below the valley floor. Between the Harwoods gauging station (near Upper Takaka) and the Spring Brook confluence, the river flows over the unconfined part of the Arthur Marble Aquifer and recharges the aquifer through gravel covered sinks. Mueller estimated the average loss from the river to be 11 000 l/s for the reach between Harwoods and Spring Brook confluence. Edgar (1998, Sect. 3) reduced the estimate to 8000–9000 l/s. A re-examination of the Takaka River gauging data (P. White, personal communication, 2001) has shown that the Harwoods to Lindsays Bridge reach loses 750 l/s and the Lindsays Bridge to Spring Brook confluence reach loses 7600 l/s, giving total recharge to the underlying aquifers of 8350 l/s on average.

Recharge from rainfall on the Takaka Valley floor occurs between Upper Takaka and Hamama (an area of about 73 km<sup>2</sup>). Major areas of recharge are the higher river terraces west of the Takaka River, and solution dolines or sinkholes are common in the area. Mueller (1992) estimated that 50% of this rainfall recharges the Arthur Marble Aquifer giving 2200 l/s. Edgar’s (1998, Sect. 3) estimate was 2200–4000 l/s, but some of this was for precipitation on the karst plateau (east of the Takaka Valley, see Section B in Fig. 2), which is included in the karst uplands contribution in Mueller’s and our models. Our estimate is 2200 l/s.

Table 1 summarises Mueller’s, Edgar’s and our estimates of recharge to the Arthur Marble Aquifer. Total recharge was 23 400 l/s in the Mueller model, of which he considered that 15 000 l/s was discharged by the Pupu Springs, and 8400 l/s by submarine springs in Golden Bay. Recharge was 14 700–20 000 l/s in the Edgar (Sect. 3) model; the lower limit (given in the table) suggests that there are no submarine springs (Doyle and Edgar, 1998). Our estimate gives recharge of 19 750 l/s, and requires that there

be submarine springs to account for the excess of recharge over discharge.

Known discharges from the Arthur Marble Aquifer are mainly via the Waikoropupu Springs. Mean discharge from the Main Spring complex was 10 000 l/s, with minimum and maximum flows of 7312 and 12 459 l/s between 1990 and 1997 (Edgar, 1998).

5 Flow from the Fish Creek Springs was 3300 l/s, with minimum and maximum flows of 53 and 6961 l/s. Other much smaller springs are known in the Takaka Valley (shown by small black dots in Fig. 1), of which Spring Brook is the most significant. (Spring Brook comprises a stream as well as seepages, whose flows have not been measured independently of the stream.) Three submarine springs are known to exist in Golden Bay, but their flows have not been measured (Williams, 2004), and subsequent investigations have not given further information (Doyle and Edgar, 1998).

#### 4.2 Constraints on recharge sources: oxygen isotopes

The average  $\delta^{18}\text{O}$  values of the three recharge sources are estimated from available data. Samples were collected at monthly intervals for three and a half years from eight locations in the Takaka Valley (Stewart and Williams, 1981; Table 2). This is long enough to give reasonable averages for the  $\delta^{18}\text{O}$  values of these features. Sampling sites (given in Fig. 1) were as follows:

1. Upper Takaka River, sampled at Harwoods gauging station.
2. Ironstone Creek (a spring-sourced perennial Takaka River tributary from the karst uplands on the east side of the valley).
3. Low's bore (groundwater from Arthur Marble in the Central Valley region, where the Takaka River loses much of its flow).
4. CTWB, previously known as Hodgkinson's bore (groundwater from the Takaka Limestone Aquifer).
5. Dairy Co. bore (groundwater from the Quaternary gravel aquifer (TTG) in the Lower Valley),

## Conceptual flow model for karst springs

M. K. Stewart and  
J. T. Thomas

Title Page

Abstract

Introduction

Conclusions

References

Tables

Figures

⏪

⏩

◀

▶

Back

Close

Full Screen / Esc

Printer-friendly Version

Interactive Discussion

6. Waikoropupu Main Spring.

7. Fish Spring (one of the Fish Creek Springs).

8. Bulk monthly rainfall samples from a rainfall collector sited at the Pupu Springs.

The Upper Takaka River (1) was sampled before any losses had occurred to the underlying aquifers. The annual mean  $\delta^{18}\text{O}$  value was quite consistent from year to year and averaged  $-8.67\text{‰}$ . The Upper Takaka River has the lowest  $\delta^{18}\text{O}$  value of any of the rivers. This results from rainout of the westerly-dominated weather systems causing the  $\delta^{18}\text{O}$  values to become progressively more negative from west to east (i.e. from the Anatoki ( $-6.5\text{‰}$ ), to the Waingaro ( $-7.2\text{‰}$ ), to the Upper Takaka ( $-8.7\text{‰}$ ) catchments). The mean  $\delta^{18}\text{O}$  of recharge from the river will be close to that of the river itself, because the recharge travels via concentrated inputs (gravel covered sinks) into the aquifer and its amount is independent of river flow when the river does not run dry. (Much of the excess, which flows out to Golden Bay, occurs during winter.) Weighting the  $\delta^{18}\text{O}$  values with the river losses to the underlying aquifer gives a weighted mean  $\delta^{18}\text{O}$  of  $-8.65\text{‰}$ , in agreement with the average value. The average  $\delta^{18}\text{O}$  for Upper Takaka River recharge is taken to be  $-8.67\text{‰}$  (Table 4).

The spring-fed Ironstone Creek (2) has a perennial flow unlike most of the other karst upland streams from east and west of the valley. The average  $\delta^{18}\text{O}$  value is  $-7.77\text{‰}$ . Low's bore (3) penetrates Arthur Marble in the mid-valley region east of the Takaka River (Fig. 1). Its average  $\delta^{18}\text{O}$  value is  $-7.94\text{‰}$ , and reflects karst upland and Upper Takaka River input. Other miscellaneous bore samples from East Takaka (samples 11–14, Table 3 and Fig. 4b) are sourced from east of the valley and had values near  $-6.9\text{‰}$ . Samples from streams west of the valley were also close to  $-7.0\text{‰}$ . On the basis of available data, the eastern tributaries have been assigned a mean  $\delta^{18}\text{O}$  of  $-7.4\text{‰}$  and the western tributaries  $-7.0\text{‰}$ , making the overall mean  $-7.2\text{‰}$ . The Waingaro and Anatoki Rivers have mean values of  $-7.2\text{‰}$  and  $-6.5\text{‰}$ , respectively. Recharge from the karst upland tributary streams is mainly via concentrated inputs (gravel covered sinkholes), and the excess during the largest flows is shed when the waters reach the

## Conceptual flow model for karst springs

M. K. Stewart and  
J. T. Thomas

Title Page

Abstract

Introduction

Conclusions

References

Tables

Figures

◀

▶

◀

▶

Back

Close

Full Screen / Esc

Printer-friendly Version

Interactive Discussion

Takaka River. The average  $\delta^{18}\text{O}$  for karst uplands recharge is taken to be  $-7.2\%$  (Table 4).

The CTWB (4), which draws water from Takaka Limestone, has an average  $\delta^{18}\text{O}$  value of  $-6.24\%$ , showing that it is sourced almost entirely from valley rainfall. Samples from bores which draw on valley rainfall-recharged groundwater (samples 15–19, Table 3 and Fig. 4b) had an average  $\delta^{18}\text{O}$  of  $-5.7\%$ . Bulk monthly rainfall (8) was collected at a raingauge at the Pupu Springs. Rainfall amounts are high, being 2000–3000 mm per year. The amount-weighted mean annual  $\delta^{18}\text{O}$  value is  $-5.82\%$ . Evapotranspiration will cause preferential selection of winter rainfall leading to a more negative average  $\delta^{18}\text{O}$  value; the corrected  $\delta^{18}\text{O}$  is  $-6.09\%$ . Recharge from rainfall on the Central Takaka Valley is via diffuse and concentrated (sinkhole) pathways. The average  $\delta^{18}\text{O}$  for valley rainfall recharge is taken to be  $-6.0\%$  (Table 4).

In the Lower Valley, the Dairy Co. bore (5) has quite negative  $\delta^{18}\text{O}$  ( $-8.23\%$ ) like the Takaka River. Both its hydrogeological situation and  $\delta^{18}\text{O}$  value suggest that the gravel aquifer here gains water from the Takaka River. However, in this reach the Takaka River has a large contribution from the Waingaro River (with mean  $\delta^{18}\text{O}$  of  $-7.2\%$ ), because so much of the Takaka flow is lost to sinks in its riverbed upstream of this point.

Samples were collected each month from both the Pupu Main Spring (6) and Fish Spring (7). A consistent difference in  $\delta^{18}\text{O}$  is found between them, with the Main Spring having higher (i.e. less negative)  $\delta^{18}\text{O}$ . The annual mean values are  $-7.38\%$  and  $-7.64\%$  respectively (Table 2). (A Student's t-test shows that the probability of these not being different is 0%.) This means that the Main Spring and Fish Spring waters contain different proportions of the source waters, and in particular Fish Spring contains more Upper Takaka River water than the Main Spring. The different proportions of the source waters in each spring are also reflected in their different chemical compositions and residence times, as seen below.

When the Pupu Springs outflow decreases and the Fish Creek Springs nearly cease to flow, because of dry conditions, the  $\delta^{18}\text{O}$  and chemical composition of the Main Spring water become more like those of Fish Spring (Stewart and Downes, 1981).

## Conceptual flow model for karst springs

M. K. Stewart and  
J. T. Thomas

Title Page

Abstract

Introduction

Conclusions

References

Tables

Figures

⏪

⏩

◀

▶

Back

Close

Full Screen / Esc

Printer-friendly Version

Interactive Discussion

This shows that at such times the Main Spring draws on similar sources to Fish Spring, and suggests that the AMA is stratified.

The mean  $\delta^{18}\text{O}$  values of the inputs and outputs to the Arthur Marble system given above allow the mass balance of  $^{18}\text{O}$  to be calculated (Table 4). The Mueller and Edgar recharge models give flow-weighted mean  $\delta^{18}\text{O}$  values of  $-7.78\text{‰}$  and  $-7.82\text{‰}$  respectively for the springs' outflow (Table 4). These do not agree with the measured values for either the Main Spring ( $-7.38\text{‰}$ ) or Fish Spring ( $-7.64\text{‰}$ ), and therefore the models cannot be correct.

Our (more complex) model matches the observed  $\delta^{18}\text{O}$  values of the Pupu Main Spring and Fish Spring, while observing the restrictions imposed by the measured input and output flows. The highlighted quantities in Table 4 are the constraints that have to be met by a satisfactory model. It is found that neither the flows nor the mean  $\delta^{18}\text{O}$  values of the springs can be matched if they are the only major outflows from the AMA system. An extra outflow of 6450 l/s, with a  $\delta^{18}\text{O}$  value of  $-8.19\text{‰}$ , is required (labelled "remainder" in Table 4) to complete the  $^{18}\text{O}$  balance. The  $\delta^{18}\text{O}$  value shows that most (75%) of the remainder must be from the Upper Takaka River (Table 4). Much of this flow is believed to be being discharged offshore via submarine springs or seepages through the seabed, because no other large outflows from the system are known. (Some small springs (of which Spring Brook is the largest, Edgar, 1998) occur between the mid-valley and the sea, but these are clearly insufficient to take the predicted flow.)

### 4.3 Chemical compositions

The chemical compositions of some waters from the Takaka Valley are given in Table 5. The rivers, springs and bores were sampled in 1979 (Stewart and Downes, 1981). Two major trends dominate the water compositions. These are 1) interaction with carbonate rocks (marble and/or limestone), and 2) addition of sea water. More subtle interactions with the other rocks tend to be masked by these trends.

Elevated concentrations of Ca,  $\text{HCO}_3$  and Sr show the effects of interaction with

**Conceptual flow  
model for karst  
springs**

M. K. Stewart and  
J. T. Thomas

Title Page

Abstract

Introduction

Conclusions

References

Tables

Figures

⏪

⏩

◀

▶

Back

Close

Full Screen / Esc

Printer-friendly Version

Interactive Discussion



carbonate rocks (samples from Ironstone Creek, Low's bore, CTWB, Main Spring and Fish Spring in Table 5). These waters are derived from Arthur Marble catchments or aquifers, except CTWB bore water which is from Takaka Limestone. Waters showing much less enrichment in Ca, etc. are the Upper Takaka River and Dairy Co. bore, which derive water from non-carbonate rocks such as schist and granite. The Dairy Co. bore is in gravel probably recharged by the Takaka River.

Elevated Na, K, Mg, Cl and SO<sub>4</sub> concentrations in the Pupu Springs and Fish Creek Springs reveal seawater input (Michaelis, 1976; Stewart and Downes, 1981). Cl concentrations show that the Pupu Main Spring water contains 0.5% sea water on average (amounting to 50 l/s in the average flow), Dancing Sands spring 0.4% and Fish Creek Springs 0.1%. However, the seawater content of Main Spring water varies between 0.2% at low flow and 0.65% at high flow (see Fig. 5a). (Figure 5a shows the total flow from the springs plus a small stream versus the Cl concentration in the Main Spring. The line gives the approximate flow from the springs if the stream water is removed.) Seawater discharge is 16 l/s from the Main Spring during the lowest flow, and 80 L/s during the highest flow, a five-fold increase. Fish Creek Springs discharge 3 l/s of seawater on average.

The  $\delta^{18}\text{O}$  values of the Main Spring also vary with flow like the Cl concentrations. Figure 5b shows the relationship between  $\delta^{18}\text{O}$  and Cl. The approximately linear relationship indicates that the Main Spring can be considered to be fed by two main water components, whose proportions vary with discharge from the spring. The components are deep system water with  $\delta^{18}\text{O} = -7.2\text{‰}$  and high Cl, and shallow system water with  $\delta^{18}\text{O} = -7.9\text{‰}$  and low Cl. The  $\delta^{18}\text{O}$  value of the shallow water is the weighted mean of the contributions from Upper Takaka River and valley rainfall to the Main Spring (Table 4). (The logic for and nature of these components are described further below.) The Main Spring points plot on the mixing line between the two components within experimental error (standard deviation of the  $\delta^{18}\text{O}$  values around the line is  $\pm 0.10\text{‰}$ ). The average values for the Main Spring and Fish Spring are also shown on the figure.

Figure 5c shows the (average) mean residence times of the Main Spring, Fish Spring

## Conceptual flow model for karst springs

M. K. Stewart and  
J. T. Thomas

Title Page

Abstract

Introduction

Conclusions

References

Tables

Figures

⏪

⏩

◀

▶

Back

Close

Full Screen / Esc

Printer-friendly Version

Interactive Discussion

and two water components versus chloride concentrations, from the residence time determinations described below. The relationships between flows, chloride,  $\delta^{18}\text{O}$  and ages (Table 6) make it clear that the Main Spring water age decreases as its flow decreases, despite the age not being able to be determined on individual samples at different flows, i.e. as the flow from the Main Spring decreases, so the contribution of deep system water will decrease, and therefore the age of the Main Spring water. This is contrary to the findings of most studies looking at the ages of springs (e.g. Siegenthaler et al., 1984).

#### 4.4 Residence time estimation: Tritium and CFCs

Reliable interpretation of the tritium ages of the springs requires that the input of tritium to the groundwater aquifer be known. This involves knowing both the tritium concentration in the precipitation and how it is affected during recharge to the AMA. Tritium concentration in precipitation is taken from monthly measurements at Kaitoke near Wellington, adjusted by a scale factor. (The scale factor adjusts precipitation data for well-known latitudinal and altitudinal variations over New Zealand, Stewart and Taylor, 1981).

The latitudes of Kaitoke and Takaka Valley are both close to  $41^{\circ}00' \text{ S}$ , and both are within mountainous terrain affected by the dominant westerlies (see inset in Fig. 1). Kaitoke is at 180 m altitude (all altitudes are given relative to mean sea level), but the precipitation-weighted mean altitude of the catchment of the Hutt River at Kaitoke was estimated to be 610 m (Stewart et al., 1983) and this is taken as the appropriate altitude affecting the precipitation. The Pupu Springs are at 14 m altitude, and the precipitation-weighted mean altitudes of the Upper Takaka River, karst uplands and valley rainfall catchment areas are estimated to be 1100 m, 460 m and 100 m, respectively. Applying the recharge model in Table 4 gives mean altitudes of recharge of 546 m for Main Spring and 690 m for Fish Spring, both similar to that at Kaitoke and indicating that the scale factor should be taken as 1.0.

The effect of the recharge process (i.e. seasonal selection of precipitation) on the

## Conceptual flow model for karst springs

M. K. Stewart and  
J. T. Thomas

Title Page

Abstract

Introduction

Conclusions

References

Tables

Figures

⏪

⏩

◀

▶

Back

Close

Full Screen / Esc

Printer-friendly Version

Interactive Discussion

isotopic composition of infiltrated water has been considered for  $^{18}\text{O}$  (both in estimating the average values above, and for the individual monthly values below). The effect is much greater for the monthly  $^{18}\text{O}$  values than for the annual tritium values. This is because using the annual means instead of the monthly tritium data smooths the seasonal selection effect of the spring tritium peak (Stewart and Taylor, 1981). Also as noted for  $^{18}\text{O}$ , the dominant recharge is from the karst uplands and Upper Takaka River, and is mainly via concentrated inputs (sinks). Consequently, the effect of seasonal selection via evapotranspiration will be small. Finally, any effect tends to be counteracted by peak flows reaching the ends of the streams more frequently in winter, which acts to produce a more constant amount of recharge through the year. Recharge from valley rainfall, which is subject to evapotranspiration, is a relatively small contributor to the AMA. For these reasons, the effect is taken as negligible.

Chlorofluorocarbons or CFCs are entirely man-made contaminants of the atmosphere and hydrological systems. Their concentrations in the atmosphere gradually increased from zero in 1940 to peaks in the early 1990s (Plummer and Busenberg, 2001). Because the gases (CFC-11 and CFC-12) are relatively long-lived, they are widely distributed in the atmosphere. CFCs are slightly soluble in water and enter groundwater systems along with water during recharge. Assuming that they were in solubility equilibrium, their concentrations in groundwater record the atmospheric concentrations when the water was recharged, thus allowing the recharge date of the water to be determined. The temperature and atmospheric pressure (i.e. altitude) during recharge need to be known.

The concentrations of the gases in groundwater can also be affected by several other processes, which can make age interpretation complicated (Plummer and Busenberg, 2001). The most important of these in the present context are:

1. Degradation or absorption in anaerobic conditions underground (CFC-11 is more susceptible to this than CFC-12). This has not been observed in the present data.
2. Contamination from local sources such as organic liquids (CFC-12 is more prone

## Conceptual flow model for karst springs

M. K. Stewart and  
J. T. Thomas

Title Page

Abstract

Introduction

Conclusions

References

Tables

Figures

⏪

⏩

◀

▶

Back

Close

Full Screen / Esc

Printer-friendly Version

Interactive Discussion

**Conceptual flow model for karst springs**

M. K. Stewart and J. T. Thomas

Title Page

Abstract

Introduction

Conclusions

References

Tables

Figures

⏪

⏩

◀

▶

Back

Close

Full Screen / Esc

Printer-friendly Version

Interactive Discussion

to this than CFC-11). This has also not been observed in the present data.

3. Presence of excess air in solution (CFC-12 is mildly sensitive to this, and CFC-11 much less). We have assumed that there is no excess air in the present samples. If excess air was present, this assumption would have caused our estimated ages to be too young.
4. Unsaturated zone effect: CFCs could travel more rapidly through the unsaturated zone than tritium, because gases can travel in the soil gas phase while tritium travels with water. This means that gas ages could be expected to be younger than tritium ages in systems with substantial unsaturated zones. However, much of the recharge in this catchment occurs via sinks and sinkholes, so this is unlikely to be a problem for these samples.

4.4.1 Main spring

Measurements of tritium concentrations in the Pupu Springs and other waters are given in Table 6. Tritium measurements for the Main Spring span 40 years, almost covering the rise and fall of tritium concentration in the atmosphere due to testing of nuclear weapons in the 1950s and 1960s. Consequently, the problem of determining the mean residence time (MRT) from tritium is well-constrained. The Main Spring accumulates water from a large area and from a wide variety of sources, so it is expected that the water will have a wide distribution of residence times. Three such mixing models have been applied to interpret the tritium age.

The mixing models are the exponential piston flow (EPM), dispersion (DM) and double dispersion (DDM) models. The DDM model is based on the 2-component flow system inferred from the  $\delta^{18}\text{O}$  and Cl measurements above.

Figure 6a shows the tritium concentrations in the recharge, the data for the Main Spring, and the best-fitting model simulations. The residence time distributions of the models (Fig. 6b) have very similar shapes with peaks of very young water and long tails of much older water. The variation of the quality of the fits with MRT is shown in

Fig. 6c, with the goodness-of-fit being expressed as the standard of deviation (sd) of the measurements about the simulations. (For the DDM model, the overall MRT was varied by changing the MRT of the deep component.)

All three models give good fits to the data, and the mean residence times are sharply constrained close to 8 years despite the larger errors in the early tritium measurements (because there were large variations in the tritium input from year to year at that time). The best EPM model has mean residence time (MRT) of 7.9 yr, exponential fraction (f) of 0.95 (i.e. it is close to an exponential model), and goodness-of-fit (sd) of  $\pm 0.40$  TU. The best DM model has MRT 8.2 yr, dispersion parameter (DP) of 1.8, and sd of  $\pm 0.29$  TU. Its age distribution is almost the same as that of the DDM model, except for the smaller peak of very young water. The best fitting DDM model fits very well indeed (sd is  $\pm 0.08$  TU). It has an overall MRT of 7.9 yr, with 74% of the water being 10.2 years old and 26% being 1.2 years old. The parameters of the DDM model are given in Table 8.

Note that the MRT determined is an average, because the MRT is expected to vary with flow (Fig. 5). The chloride values for the Main Spring (Table 7) give an indication of the flow when the spring was sampled. Mean Cl for the Main Spring was 95 mg/l (Table 6), so the 1966 sample was sampled during above average flow, the 1972 and 1976 samples during average flows and the 1999 sample during less than average flow.

CFC measurements are given in Table 7. CFC measurements have given useful information on water residence times in a number of New Zealand groundwater systems (Stewart and Morgenstern, 2001). We have found that groundwater ages estimated using CFC-11 and tritium are often in agreement, whereas ages estimated using CFC-12 are generally several years younger. CFC samples were collected in 1998 and 2000. For CFC-11, applying the EPM( $f=0.95$ ) model gives the best-fit MRT of 12.2 yr, and the DM( $DP=1.8$ ) model MRT of 4.8 yr, both quite different from each other and from the tritium result. Applying the DDM model with the same water components as for tritium, but optimising the fit by varying the young fraction (b), gives a best-fit model with

## Conceptual flow model for karst springs

M. K. Stewart and  
J. T. Thomas

Title Page

Abstract

Introduction

Conclusions

References

Tables

Figures

⏪

⏩

◀

▶

Back

Close

Full Screen / Esc

Printer-friendly Version

Interactive Discussion

$b=0.24$  and overall MRT of 8.0 yr, very similar to that for tritium. This suggests that the DDM age distribution has more validity in this system than the other two models (EPM and DM), and supports the conceptual model below. Model parameters are given in Table 8.

For CFC-12, the best-fit MRTs with the same models (i.e. keeping the other parameters the same) are 9.2 yr, 3.2 yr and 5.7 yr ( $b=0.50$ ), respectively. None of these agree well with the results for tritium and CFC-11. This is consistent with our previous observations that CFC-12 frequently gives younger residence times than tritium and CFC-11 (Stewart and Morgenstern, 2001).

To compare the sensitivities of the tritium result with the CFC results we have plotted the goodness-of-fit (sd) divided by the measurement error ( $\epsilon$ ) against  $b$  in Fig. 7a. (For tritium, the error has been taken as the root mean square of the first three measurements when the quoted errors were much larger than for the later samples.) The best-fit values of  $b$  for tritium and CFC-11 are close to the value calculated from the recharge flows in Table 4 (shown by the dashed vertical line in Fig. 7a). As noted, the CFC-12 value is quite different and has been disregarded.

#### 4.4.2 Fish Spring

Fish Spring results are given in Table 7. The EPM and DM models with broad distributions are not effective for estimating the ages of the Fish Spring (fits are poor and/or the ages are not consistent with each other), but the DDM model appears to work well. Applying the DDM model to tritium and allowing the young fraction to vary gives a best-fit model with  $b=0.67$  (Fig. 7b). However, the discrimination is weak with only one measurement, so  $b$  could lie within a range of at least  $\pm 0.2$ . Applying the model to the two CFC-11 measurements gives a best fit at  $b=0.81$ ; this is estimated to have an error of about  $\pm 0.1$ . With CFC-12, the best-fit model is  $b=0.70$ . These are all relatively close to the value calculated from the recharge flows in Table 4 (i.e.  $b=0.75$ , shown by the dashed vertical line in Fig. 7b). In this case, the CFC-12 measurements appear to have given an acceptable result (unlike for the Main Spring). This is possibly due to the

## Conceptual flow model for karst springs

M. K. Stewart and  
J. T. Thomas

Title Page

Abstract

Introduction

Conclusions

References

Tables

Figures

⏪

⏩

◀

▶

Back

Close

Full Screen / Esc

Printer-friendly Version

Interactive Discussion

dominance of the younger component in Fish Spring water.

#### 4.4.3 Balls bore

Balls bore (WWD 6011) is a deep well (114 m) with a long unscreened interval located approximately 425 m southwest of the Main Spring (Fig. 3). The bore penetrates 33 m of Motupipi Coal Measures before encountering fractured Arthur Marble, and is cased to 35 m depth. The ground level is 21 m a.s.l. compared with 14 m at the Main Spring and 17 m at Fish Spring. Rest water level (with no pumping) in the bore is 18 m a.s.l.

The  $\delta^{18}\text{O}$  value of the water is  $-6.48\%$ , indicating a dominance of valley rainfall and likely absence of Upper Takaka River water. Tritium and CFC results are given in Table 7. To obtain a consistent age from the tritium and CFC measurements, R. van der Raaij (personal communication, 2006) found he had to assume binary mixing of two source waters. The mixture comprised approximately two thirds of 1-yr-old water (assumed to be from shallow level) and one third of much older water (containing zero tritium and CFCs and therefore probably at least 100-yr-old) from depth. The  $\delta^{18}\text{O}$  value is consistent with two thirds 1-yr-old water being sourced from valley rainfall, and one third 100-yr-old water from karst uplands.

The result is interesting, because it emphasises how laterally inhomogeneous and stratified the AMA is. Clearly waters with very different residence times and sources can be drawn from different parts of the aquifer. The 1-yr-old shallow water component is like that observed at the Pupu Springs, but with a different source. The 100-yr-old water is likely to be from the porous matrix reflecting the fact that there is no natural outflow and few or much smaller deep fissures at this site. (e.g. Drawdown with pumping is considerable, being 3.2 m with 10.7 l/s water extraction.)

#### 4.5 Residence time estimation of the shallow component: oxygen-18 variations

The  $\delta^{18}\text{O}$  variations in the Main and Fish Springs can be used to estimate the mean residence time of the shallow component (MRT about 1.2 yr). The deep component

## Conceptual flow model for karst springs

M. K. Stewart and  
J. T. Thomas

Title Page

Abstract

Introduction

Conclusions

References

Tables

Figures

⏪

⏩

◀

▶

Back

Close

Full Screen / Esc

Printer-friendly Version

Interactive Discussion



(MRT=10.2 yr) has too long a residence time to show any variations due to the  $\delta^{18}\text{O}$  variations in its input water, so its  $\delta^{18}\text{O}$  value can be assumed to be constant at  $\delta^{18}\text{O} = -7.2\text{‰}$ . But the shallow component water should be young enough to show effects from the  $\delta^{18}\text{O}$  variations of its inputs.

The input  $\delta^{18}\text{O}$  values of the shallow system can be calculated by correcting the valley rainfall data (site 8) for evapotranspiration and the Upper Takaka River data (site 1) for river flow by the method described in Stewart et al. (2007). The calculations use the weighting formula given by Bergmann et al. (1986)

$$\delta_w = \frac{R_i}{R_{\text{mean}}}(\delta_i - \delta_{\text{mean}}) + \delta_{\text{mean}} \quad (6)$$

where  $\delta_w$ ,  $\delta_i$  are the weighted and measured  $\delta^{18}\text{O}$  values, and  $R_i$  the groundwater recharge amount, in the  $i$ th month respectively.  $\delta_{\text{mean}}$  and  $R_{\text{mean}}$  are the mean  $\delta^{18}\text{O}$  values and recharge amounts.

The  $\delta^{18}\text{O}$  values of the recharge for Main Spring are given by

$$\delta_{\text{MSrech}} = b(0.29\delta_{\text{wrf}} + 0.71\delta_{\text{wUTR}}) + (1 - b)\delta_{\text{wku}} \quad (7)$$

and that for Fish Spring is

$$\delta_{\text{FSrech}} = b(0.33\delta_{\text{wrf}} + 0.67\delta_{\text{wUTR}}) + (1 - b)\delta_{\text{wku}} \quad (8)$$

where  $b$  is the shallow fraction, and  $\delta_{\text{wrf}}$ ,  $\delta_{\text{wUTR}}$ ,  $\delta_{\text{wku}}$  are the weighted  $\delta^{18}\text{O}$  values for valley rainfall, Upper Takaka River and karst uplands ( $-7.2\text{‰}$ ), respectively, from Eq. (6). The multiplying factors are the ratios of the flows in Table 4. Figure 8a shows the calculated  $\delta^{18}\text{O}$  variations in the recharge for the two springs.

Three adjustable parameters were used to simulate the  $\delta^{18}\text{O}$  values of the Main Spring, namely the MRT and DP of the shallow water, and  $b$ . The variation of the goodness-of-fit parameter with MRT is shown in Fig. 8b, and the best-fitting simulation is given in Fig. 8c. (The first 12 measurements were omitted because they would

## Conceptual flow model for karst springs

M. K. Stewart and  
J. T. Thomas

Title Page

Abstract

Introduction

Conclusions

References

Tables

Figures

◀

▶

◀

▶

Back

Close

Full Screen / Esc

Printer-friendly Version

Interactive Discussion



have been affected by recharge before the measurements on valley rainfall and Upper Takaka River had begun.) The best fit is obtained with  $MRT=1.0$  yr,  $DP=0.1$  and  $b=0.3$ , which are all close to the values obtained from the earlier work (i.e.  $MRT=1.2$  yr,  $DP=0.12$ ,  $b=0.26$ ). This gives good support to the 2-component model.

The same three parameters were used to fit the  $\delta^{18}O$  values of the Fish Spring. The optimum fit is obtained with  $MRT=1.1$  yr,  $DP=0.3$ ,  $b=0.75$  (Figs. 8b, d). These also agree well with the parameters from the earlier work ( $MRT=1.2$  yr,  $DP=0.12$ ,  $b=0.75$ ).

The variation of the quality of fit with  $b$  is compared with those for tritium and CFCs in Figs. 7a, b. The optimum fits occur at close to the same values of  $b$  as with the other tracers, and therefore strongly support the 2-component model for the springs, and in particular the existence of the shallow component with  $MRT$  about 1.2 yr.

One source of error in the estimation of the  $\delta^{18}O$  values of the recharge to the springs is the assumption that  $b$  and the proportions of Upper Takaka River and valley rainfall waters are constant. In fact, these are likely to vary in time as the catchment wetness and therefore spring flow varies.

## 5 Discussion

### 5.1 Karst hydrology

Karst landscapes are produced by groundwaters percolating through limestone rock and gradually dissolving the carbonate minerals. Limestones are commonly well-jointed, and water initially penetrates slowly along joints. In time, solution of carbonate minerals by the water gradually widens the joints into fissures. Eventually an interconnected system of solution cavities forms allowing water to move easily from sinks in the recharge area through the rock to emerge as springs at the foot of the catchment.

Arthur Marble is a thermally metamorphosed limestone produced by recrystallisation of the constituent carbonate grains. The development of a crystalline matrix will have reduced the primary matrix porosity of the original limestone, and solution of the joints

## Conceptual flow model for karst springs

M. K. Stewart and  
J. T. Thomas

Title Page

Abstract

Introduction

Conclusions

References

Tables

Figures

◀

▶

◀

▶

Back

Close

Full Screen / Esc

Printer-friendly Version

Interactive Discussion

will have enhanced the secondary fissure porosity. Consequently, the rates of flow in the two media of pores and solution cavities will differ by orders of magnitude producing a markedly dual porosity aquifer.

The idea of karst hydrology being controlled by two integrated subsystems with different porosities (representing fissured-porous matrix and solution cavities respectively) has been used very widely in karst studies (e.g. page 1, Ford and Williams, 1989), and has been applied to interpret tritium and oxygen-18 measurements in karst springs by Rank et al. (1992); Maloszewski et al. (2002). Figure 9a (adapted from Maloszewski et al., 2002) illustrates the nature of flow in karst aquifers. Connected porosity occurs in small-scale fissures and porous matrix of the marble providing the majority of the storage in the system (the fissured-porous aquifer), and a low-volume but high-velocity conduit system (karstic channels) conveys water from entrances to exits while interacting with water in the pores on the way.

## 5.2 Conceptual model of the Arthur Marble Aquifer Flow System

The conceptual model presented here (Fig. 9b), however, is different. It is based on the measurements and deductions described above. The AMA flow system supplying the Waikoropupu Springs is conceived of as containing two flow systems, each being dual porosity aquifers like that illustrated schematically in Fig. 9a. Springs generally draw on deeper groundwater sources during low flow conditions, with the water becoming older as flow decreases. And, in particular, springs fed by the dual porosity aquifer of Fig. 9a would become older with decreasing flow because more of the water would come from the porous matrix. However, with the Waikoropupu Springs the opposite happens, the water becomes younger as flow decreases (Fig. 5). This leads logically to the idea of two flow systems with different recharge sources.

The deep system supplies the majority of the flow to the Main Spring complex via one or more major fissures or solution channels, which connect the deep fissure network to the springs. The system includes the deep parts of the marble below the Takaka Valley floor and the marble on both sides of the valley. The marble outcrops on the

## Conceptual flow model for karst springs

M. K. Stewart and  
J. T. Thomas

Title Page

Abstract

Introduction

Conclusions

References

Tables

Figures

⏪

⏩

◀

▶

Back

Close

Full Screen / Esc

Printer-friendly Version

Interactive Discussion

sides of the valley show strong evidence of karstification, based on surface expression and the presence of caves (with the most famous cave being Harwood's Hole with a 183 m vertical drop). The marble beneath the valley will also have been karstified down to at least 130 m during lower sea-level stands. <sup>18</sup>O evidence shows that recharge for the deep water component is from the small tributary streams and rainfall on the karst uplands on each side of the valley. The pressure from the higher water tables on the sides of the valley (especially the karst plateau on the east side), transmitted by the solution channel network, plus the confining layer in the lower valley, produce high piezometric levels in the confined area. Most of the deep system recharge eventually emerges at the Main Spring complex where the confining layer thins – about 80% of the water entering the deep system is discharged by the Main Spring complex on average (Table 4). Lesser amounts emerge in the Fish Creek Springs (9%) and the rest can probably be accounted for by seepages upwards into the mostly overlying shallow system. Hence, it is unlikely that much water escapes into the sea from the deep system in spite of the evident presence of sea water at depth in the aquifer. The source of the sea water is believed to be present-day infiltration (possibly by a venturi effect, Williams, 1977; Fleury et al., 2007), although presence of remnant or fossil sea water from an earlier incursion of sea water or even operation of a complex ion exchange-diffusion process through a sediment interface cannot be entirely ruled out. The powerful upflow in the deep system near the springs carries sea water from depth into the springs' discharge.

The mean residence time of the deep water (measured in the Main Spring) is long (10.2 yr) and the storage capacity of the aquifer very large (water volume estimated from flow times age =  $9200 \text{ l/s} \times 10.2 \text{ yr} = 3.0 \text{ km}^3$ ). Much of the saturated part of the system is below sea level. Interaction between channel network water and fissured-porous matrix water may affect the chemical and isotopic concentrations of the channel water (e.g. Elliot et al., 1999), although the marble probably has a very low porosity. There is possibly much older water resident in less accessible parts of the porous matrix, as shown by the results for Balls bore.

## Conceptual flow model for karst springs

M. K. Stewart and  
J. T. Thomas

Title Page

Abstract

Introduction

Conclusions

References

Tables

Figures

◀

▶

◀

▶

Back

Close

Full Screen / Esc

Printer-friendly Version

Interactive Discussion

The shallow system underlies the Takaka Valley. The unconfined part in the Central Valley includes Arthur Marble, Takaka Limestone and Takaka Gravel, while the confined part in the Lower Valley is in Arthur Marble beneath the Motupipi Coal Measures. Recharge is from both the Upper Takaka River and valley rainfall. Much of the water (52%) bypasses the Pupu Springs and is discharged offshore in springs and seeps, some (25%) appears in the Main Spring complex and 23% in the Fish Creek Springs (Table 4). The water discharged in the Pupu Springs is estimated to have a mean residence time of 1.2 years. The water volume estimated from flow times age is  $0.4 \text{ km}^3$ .

### 5.3 Location of the Waikoropupu Springs and the relationship between the two flow systems

A question that arises is: why do these two systems act as if they are separate, although apparently residing in the same aquifer? Williams (1977) discussed the related question of why the springs are located in a small tributary valley on the west side of the Takaka fault-angle valley, and 5 km from the line of shortest distance between the upper valley and the sea. He found this a surprising location, and considered that there must be a special local circumstance at Takaka to explain it. One of his hypothesised explanations for the location helps to shed light on the relationship between the two systems.

Williams had two alternative explanations for the location of the springs. The first was that there is a diorite intrusion in the marble at shallow levels under the Takaka Valley, which blocks water in the deep system from flowing towards the sea. The diorite, which is not shown on geological maps of the area (Rattenbury et al., 1998), was suggested by Jones (1939) from a survey of magnetic anomalies in the Takaka region. Jones's zero magnetic anomaly outline for the suggested intrusive is shown in Fig. 1. The diorite, which lies parallel to and is shown on Section A in Fig. 2, would divert water in the deep system very effectively towards the Pupu Springs in the west, while allowing the shallow system water to flow towards the sea and escape via submarine outlets. The Pupu Springs themselves, occurring where the cap rock is thinnest and artesian

## Conceptual flow model for karst springs

M. K. Stewart and  
J. T. Thomas

Title Page

Abstract

Introduction

Conclusions

References

Tables

Figures

⏪

⏩

◀

▶

Back

Close

Full Screen / Esc

Printer-friendly Version

Interactive Discussion

pressures highest, would also induce convergence of flow and draw both deep water, and a proportion of the shallow water to the springs.

The second explanation was that the marble is more limited in extent than shown in Fig. 1 and strikes in the direction of Pupu, thereby channelling the flow in that direction.

5 This is not considered a viable explanation in view of the geology and the current results.

## 6 Conclusions

The paper examines the evidence on recharge sources to the Arthur Marble Aquifer and establishes a new recharge model using the most reliable information. This recharge model is used with estimates of the average  $\delta^{18}\text{O}$  values of the three groups of recharge sources to derive an  $^{18}\text{O}$  mass balance for the inputs and outputs of the AMA by means of a spreadsheet (Table 4). The results show that the Main Spring is sourced mainly from the karst uplands (74%), with smaller contributions from the Upper Takaka River (18%) and valley rainfall (8%). In contrast, Fish Creek Springs are fed mainly by Upper Takaka River (50%), with valley rainfall (25%) and karst uplands (25%). The unexpected consequence of the mass balance is that much of the Upper Takaka River contribution to the aquifer (58%) must bypass the springs and be discharged via offshore springs and seeps.

20 The chemical concentrations of the Waikoropupu Springs reflect input of sea water, at average rates of 0.5% in the Main Spring and 0.1% in Fish Creek Springs, but varying with flow. The chloride is carried by the karst uplands-sourced deep water. Tritium measurements spanning 40 years, and CFC-11 measurements, give a mean residence time of 8 years for the Main Spring water. Fish Spring water has mean residence time of 3.5 yr. The measurements are best explained by a two-component model, with different proportions of deep (MRT 10.2 yr) and shallow (MRT 1.2 yr) components contributing to each spring. Monthly  $^{18}\text{O}$  measurements on the springs corroborate the proportions and residence time of the shallow component in the spring flows.

---

### Conceptual flow model for karst springs

M. K. Stewart and  
J. T. Thomas

---

Title Page

Abstract

Introduction

Conclusions

References

Tables

Figures

◀

▶

◀

▶

Back

Close

Full Screen / Esc

Printer-friendly Version

Interactive Discussion

**Conceptual flow model for karst springs**

M. K. Stewart and J. T. Thomas

Title Page

Abstract

Introduction

Conclusions

References

Tables

Figures

⏪

⏩

◀

▶

Back

Close

Full Screen / Esc

Printer-friendly Version

Interactive Discussion

These observations are integrated in a conceptual model of flow in the AMA (Fig. 9). The three groups of recharge sources supply two flow systems. The first is a deep aquifer, which underlies the Takaka Valley and crops out (and is recharged) on each side in the karst uplands (see cross-sections, Fig. 2). Higher water tables on the sides drive the deep flow, which bursts upwards at the Main Spring complex, discharging most (average 80%) of the karst uplands-sourced water. The mean residence time of the water is 10.2 yr giving a total aquifer volume of 3.0 km<sup>3</sup>. The powerful upflow near the springs carries sea water from depth. 10% of the karst uplands water is discharged at the Fish Creek Springs, and the rest seeps upwards into the overlying second system.

The second system is a shallow aquifer underlying the Takaka Valley. Recharge is from sinks in the bed of the Takaka River and rainfall on the valley where the AMA is unconfined. Much of the water flows downvalley and is discharged in springs offshore (52%), but some is discharged in the Main Spring complex (25%) and Fish Creek Springs (23%). The mean residence time is 1.2 yr giving aquifer volume of 0.4 km<sup>3</sup>.

The very different behaviours of the two systems are believed to be due to the presence of a diorite intrusive at shallow levels below the surface of the lower Takaka Valley. This intrusive diverts the deep water flow towards the Pupu Springs, blocking it from flowing towards the sea, and thereby separating the deep flow or system from the shallow flow or system, much of which travels over the intrusive and escapes via submarine springs.

This research has revealed two almost paradoxical results. 1. The age of the Waikopopu Springs water increases with flow (in contrast to most other springs investigated elsewhere). 2. The deep system contains infiltrated sea water but does not lose (fresh) water to the sea, while the shallow system loses (fresh) water to the sea but does not gain sea water by infiltration. A buried diorite intrusive provides a good explanation for these seeming paradoxes.

*Acknowledgements.* The authors thank U. Morgenstern and R. van der Raaij for contributing data and insight on age dating. V. Trompeter (nee Fox) is thanked for the CFC measurements.

C. B. Taylor (now deceased) is acknowledged for his contributions in developing the tritium laboratory and to understanding the Waikoropupu Springs.

## References

- Bergmann, H., Sackl, B., Maloszewski P., and Stichler, W.: Hydrological investigation in a small catchment area using isotope data series, in: Proceedings of the Fifth International Symposium on Underground Water Tracing, Institute of Geology and Mineral Exploration, Athens, 255–272, 1986.
- Busenberg, E. and Plummer, L. N.: Use of chlorofluorocarbons ( $\text{CCl}_3\text{F}$  and  $\text{CCl}_2\text{F}_2$ ) as hydro-  
10 logical tracers and age-dating tools: The alluvium and terrace system of Central Oklahoma, *Water Resour. Res.*, 28(9), 2257–2283, 1992.
- Doyle, M. and Edgar, J. E.: There are no springs in the water balance, New Zealand Hydrological Society 1998 Symposium Proceedings, p.27, Dunedin, 24–27 November 1998.
- Edgar, J. E.: Hydrogeology of the Takaka Valley, M.Sc. Thesis, University of Canterbury, 303 pp., 1998.
- 15 Elliot, T., Andrews, J. N., and Edmunds, W. M.: Hydrochemical trends, paleorecharge and groundwater ages in the fissured Chalk aquifer of the London and Berkshire Basins, U.K. *Appl. Geochem.*, 14, 333–363, 1999.
- Fleury, P., Bakalowicz, M., and de Marsily, G.: Submarine springs and coastal karst aquifers: A review, *J. Hydrol.*, 339(1–2), 79–92, doi:10.1016/j.jhydrol.2007.03.009, 2007.
- 20 Ford, D. C. and Williams, P. W.: *Karst geomorphology and Hydrology*, Chapman and Hall, London, 1989.
- Jones, W. M.: Magnetic observations in the Onekaka-Parapara District, with some remarks on the geology of the iron-ore deposits, *N.Z. J. Sci. Technol.*, 21B(1), 16–30, 1939.
- Hulston, J. R., Taylor, C. B., Lyon, G. L., Stewart, M. K., and Cox, M. A.: Environmental isotopes  
25 in New Zealand hydrology. Part 2. Standards, measurement techniques and reporting of measurements for oxygen-18, deuterium and tritium in water, *N.Z. J. Sci.*, 24, 313–322, 1981.
- IAEA: Fifth IAEA intercomparison of low-level tritium measurements in water, Report prepared by G. Östlund, E. M. Scott and C. B. Taylor for the Isotope Hydrology Section of the I.A.E.A.,  
30 Vienna, Austria, 1995.

## Conceptual flow model for karst springs

M. K. Stewart and  
J. T. Thomas

Title Page

Abstract

Introduction

Conclusions

References

Tables

Figures

◀

▶

◀

▶

Back

Close

Full Screen / Esc

Printer-friendly Version

Interactive Discussion



- Maloszewski, P. and Zuber, A.: Determining the turnover time of groundwater systems with the aid of environmental tracers, 1. Models and their applicability, *J. Hydrol.*, 57, 207–331, 1982.
- Maloszewski, P., Stichler, W., Zuber, A., and Rank, D.: Identifying the flow systems in a karstic-fissured-porous aquifer, the Schneealpe, Austria, by modelling of environmental  $^{18}\text{O}$  and  $^3\text{H}$  isotopes, *J. Hydrol.*, 256, 48–59, 2002.
- Michaelis, F. B.: Physico-chemical features of Puppu Springs, N.Z. *J. Mar. Freshwater Res.*, 10(4), 613–628, 1976.
- Morgenstern, U. and Taylor, C. B.: Low-level tritium measurement using electrolytic enrichment and liquid scintillation counting, *Proc. International Symposium on Quality Assurance for Analytical Methods in Isotope Hydrology*, Vienna, Austria, 2005.
- Mueller, M.: Karst hydrogeology of the Takaka Valley, Golden Bay, northwest Nelson, N.Z. *J. Geol. Geophys.*, 34, 11–16, 1991.
- Mueller, M.: Geohydrology of the Takaka Valley, Unpublished report, Tasman District Council, Richmond, N.Z., 1992.
- Park, J.: On the geology of Collingwood County, Nelson, New Zealand Geological Survey report of geological exploration, 20, 186–243, 1890.
- Plummer, L. N. and Busenburg, E.: Chlorofluorocarbons, Chapter 15 in *Environmental Tracers*, in: *Subsurface Hydrology*, edited by: Cook, P. and Herczeg, A. L., Kluwer Academic Publishers, pp. 441–478, 1999.
- Rapier, D.: Waikoropupu Springs – some hydrological aspects, Unpublished report, N.Z. Ministry of Works, Nelson, N.Z., 1975.
- Rattenbury, M. A., Cooper, R. A., and Johnston, M. R. (Eds.): *Geology of the Nelson Area*, IGNS 1:250,000 Geological Map 9, 1 sheet and 67 p., 1998.
- Rank, D., Völkl, G., Maloszewski, P., and Stichler, W.: Flow dynamics in an alpine karst massif studied by means of environmental isotopes, *Isotope Techniques in Water Resources Development 1991*, IAEA Symposium 319, March 1991, Vienna, pp. 327–343, 1992.
- Rosen, M. R., Cameron, S. G., Taylor, C. B., and Reeves, R. R.: New Zealand guidelines for the collection of groundwater samples for chemical and isotopic analyses, I.G.N.S. Science Report 99/9, 81 p., 1999.
- Siegenthaler, U., Schotterer, U., and Muller, I.: Isotopic and chemical investigations of springs from different karst zones in the Swiss Jura, in: *Isotope Hydrology*, 1983, 153–172, Vienna, IAEA, 1984.
- Stewart, M. K. and Downes, C. J.: Isotope hydrology of Waikoropupu Springs, New Zealand,

---

**Conceptual flow model for karst springs**

M. K. Stewart and  
J. T. Thomas

---

[Title Page](#)[Abstract](#)[Introduction](#)[Conclusions](#)[References](#)[Tables](#)[Figures](#)[⏪](#)[⏩](#)[◀](#)[▶](#)[Back](#)[Close](#)[Full Screen / Esc](#)[Printer-friendly Version](#)[Interactive Discussion](#)



- Isotope Studies of Hydrologic Processes, NIU Press, DeKalb, IL, pp. 15–23, 1981.
- Stewart, M. K. and Morgenstern, U.: Age and source of groundwater from isotope tracers, in: Groundwaters of New Zealand, edited by: Rosen, M. R. and White, P. A., New Zealand Hydrological Society Inc., Wellington, pp. 161–183, 2001.
- 5 Stewart, M. K. and Taylor, C. B.: Environmental isotopes in New Zealand hydrology. 1. Introduction: The role of oxygen 18, deuterium and tritium in hydrology, N.Z. J. Sci., 24, 295–311, 1981.
- Stewart, M. K. and Williams, P. W.: Environmental isotopes in New Zealand hydrology. 3. Isotope hydrology of Waikoropupu Springs and Takaka River, northwest Nelson, N.Z. J. Sci., 10 24, 323–337, 1981.
- Stewart, M. K., Cox, M. A., James, M. R., and Lyon, G. L.: Deuterium in New Zealand rivers and streams, I.N.S. Science Report (INS-R-320), 32 p., 1983.
- Stewart, M. K., Mehlhorn, J., and Elliott, S.: Hydrometric and natural tracer ( $^{18}\text{O}$ , silica,  $^3\text{H}$  and  $\text{SF}_6$ ) evidence for a dominant groundwater contribution to Pukemanga Stream, New Zealand, Hydrol. Processes, doi:10.1002/hyp.6557, 2007.
- 15 Taylor, C. B.: The relationship between electrolytic deuterium and tritium separation factors, and attainment of improved accuracy in radiometric low-level tritium measurement, J. Appl. Rad. Isotopes 45(6), 683–692, 1994.
- Taylor, C. B.: Contributing sources to Waikoropupu Springs, Takaka, NW Nelson: a new assessment, New Zealand Hydrological Society 2001 Symposium Proceedings, p. 38–39, Palmerston North, 20–23 November 2001.
- 20 Thomas, J.: Groundwater resources of the Tasman Region, in: Groundwaters of New Zealand, edited by: Rosen, M. R. and White, P. A., New Zealand Hydrological Society Inc., Wellington, pp. 411–425, 2000.
- 25 Williams, P. W.: Hydrology of the Waikoropupu Springs: a major tidal karst resurgence in northwest Nelson (New Zealand), J. Hydrol., 35, 73–92, 1977.
- Williams, P. W.: Karst systems, Chapter 31, in: Freshwaters of New Zealand, edited by: Harding, J. S., Mosley, M. P., Pearson, C. P., and Sorrell, B. K., N.Z. Hydrol. Soc. and N.Z. Lim. Soc., Christchurch, New Zealand, 2004.

---

**Conceptual flow  
model for karst  
springs**

M. K. Stewart and  
J. T. Thomas

---

[Title Page](#)[Abstract](#)[Introduction](#)[Conclusions](#)[References](#)[Tables](#)[Figures](#)[⏪](#)[⏩](#)[◀](#)[▶](#)[Back](#)[Close](#)[Full Screen / Esc](#)[Printer-friendly Version](#)[Interactive Discussion](#)

## Conceptual flow model for karst springs

M. K. Stewart and  
J. T. Thomas

**Table 1.** Recharge flows to the Arthur Marble Aquifer.

Source of recharge	Mueller (1992)	Edgar (1998) (min)	This work
Karst uplands (l/s)	10 200	4500	9200
Upper Takaka River (l/s)	11 000	8000	8350
Valley rainfall (l/s)	2200	2200	2200
Total recharge (l/s)	23 400	14 700	19 750

Title Page

Abstract

Introduction

Conclusions

References

Tables

Figures

⏪

⏩

◀

▶

Back

Close

Full Screen / Esc

Printer-friendly Version

Interactive Discussion

**Conceptual flow model for karst springs**

M. K. Stewart and J. T. Thomas

**Table 2.** Mean annual  $\delta^{18}\text{O}$  values of waters from the Takaka Valley.

Map ID	Feature sampled	$\delta^{18}\text{O}$ (‰)				Mean
		1976	1977	1978	1979	
1	Upper Takaka River	-8.73	-8.75	-8.66	-8.53	-8.67
2	Ironstone Creek	-7.68	-7.85	-7.88	-7.66	-7.77
3	Lows bore	-7.88	-7.97	-7.99	-7.93	-7.94
4	CTWB	-6.15	-6.24	-6.32	-6.26	-6.24
5	Dairy Co. bore	-8.13	-8.28	-8.33	-8.16	-8.23
6	Pupu Main Spring	-7.24	-7.31	-7.48	-7.50	-7.38
7	Pupu Fish Spring	-7.53	-7.67	-7.69	-7.66	-7.64
8	Rainfall (mean)	-5.41	-5.43	-5.27	-5.50	-5.40
	Rainfall (weighted)	-5.62	-5.98	-6.10	-5.59	-5.82
	Rainfall amount (mm)	2730	2178	2037		

Title Page

Abstract Introduction

Conclusions References

Tables Figures

⏪ ⏩

◀ ▶

Back Close

Full Screen / Esc

Printer-friendly Version

Interactive Discussion

**Conceptual flow model for karst springs**

M. K. Stewart and  
J. T. Thomas

**Table 3.** Miscellaneous  $\delta^{18}\text{O}$  values of groundwaters from the Takaka Valley.

Well No.	Feature Sampled (Map no. in bracket)	Aquifer	$\delta^{18}\text{O}$ (‰)		
			3/1999	2/2000	Mean
Karst uplands-sourced groundwater					
6814	Mansons bore (11)	Takaka Limestone	-6.91	-6.86	
6821	Borlase bore (12)	Takaka Limestone		-7.09	
6819	Sixtus bore (13)	Takaka Gravel	-6.50	-7.13	
6808	Moyle bore (14)	Takaka Limestone	-6.97	-6.74	$-6.9 \pm 0.2$
Valley rainfall-sourced groundwater					
S	Spring at quarry (15)	Takaka Limestone	-5.46		
6604	Bore at quarry (16)	Takaka Limestone	-5.75		
6601	CTWB (17)	Takaka Limestone	-5.56		
6323/P5	Bore Dairy Co. (18)	Takaka Limestone	-5.91		
6103	Bisley bore (19)	Takaka Gravel	-5.83		$-5.7 \pm 0.2$

Title Page

Abstract Introduction

Conclusions References

Tables Figures

⏪ ⏩

◀ ▶

Back Close

Full Screen / Esc

Printer-friendly Version

Interactive Discussion

**Conceptual flow model for karst springs**

M. K. Stewart and J. T. Thomas

**Table 4.**  $\delta^{18}\text{O}$  values of flows to and from the Arthur Marble Aquifer. The contributions from individual recharge sources to each spring were adjusted to satisfy the oxygen-18 mass balance (based on the highlighted measured quantities).

Recharge source	$\delta^{18}\text{O}$ ‰	Mueller	Edgar	Flows in this work			Total
		Flows l/s	Flows l/s	Main Spring l/s	Fish Spring l/s	Remainder l/s	Flows l/s
Karst uplands	<b>-7.20</b>	10 200	4500	7400	830	970	<b>9200</b>
Upper Takaka River	<b>-8.67</b>	11 000	8000	1850	1650	4850	<b>8350</b>
Valley rainfall	<b>-6.00</b>	2200	2200	750	820	630	<b>2200</b>
Total flows (l/s)		23 400	14 700	<b>10 000</b>	<b>3300</b>	6450	19 750
$\delta^{18}\text{O}^1$ (‰)		-7.78	-7.82	<b>-7.38</b>	<b>-7.64</b>	-8.19	-7.69
Shallow fraction <sup>2</sup> (b)		-	-	0.26	0.75	0.85	-

<sup>1</sup>Weighted means of total flows

<sup>2</sup>See conceptual model below.

Title Page

Abstract Introduction

Conclusions References

Tables Figures

◀ ▶

◀ ▶

Back Close

Full Screen / Esc

Printer-friendly Version

Interactive Discussion

## Conceptual flow model for karst springs

M. K. Stewart and  
J. T. Thomas

**Table 5.** Chemical concentrations (mg/l) in some Takaka waters (14 March 1979).

ID	Sample	Ca	HCO <sub>3</sub>	Sr	Na	K	Mg	Cl	SO <sub>4</sub>
1	Upper Takaka River	10	37	0.04	2	0.2	2.4	2.6	3
2	Ironstone Creek	47	157	0.11	4	0.5	1.3	2.1	1
3	Low's Bore	43	139	0.09	3	0.5	2.4	3.3	4
4	C T W B	42	135	0.12	6	0.5	2.7	5.6	3
5	Dairy Co. Bore	14	48	0.05	3	0.3	2.1	3.2	3
6	Pupu Main Spring	57	194	0.16	47	3.9	6.6	75	15
7	Pupu Fish Spring	43	145	0.11	12	1.5	3.4	16	6

Title Page

Abstract

Introduction

Conclusions

References

Tables

Figures

⏪

⏩

◀

▶

Back

Close

Full Screen / Esc

Printer-friendly Version

Interactive Discussion

**Conceptual flow model for karst springs**

M. K. Stewart and  
J. T. Thomas

**Table 6.** Average compositions of Waikoropupu Springs and component waters.

Sample	b	Cl mg/l	$\delta^{18}\text{O}$ ‰	MRT yr
Deep system water	0	124	-7.20	10.2
Main Spring	0.26	95	-7.38	7.9
Fish Spring	0.75	26	-7.64	3.5
Shallow system water	1	2	-7.90	1.2

Title Page

Abstract

Introduction

Conclusions

References

Tables

Figures

⏪

⏩

◀

▶

Back

Close

Full Screen / Esc

Printer-friendly Version

Interactive Discussion

## Conceptual flow model for karst springs

M. K. Stewart and  
J. T. Thomas

Title Page

Abstract

Introduction

Conclusions

References

Tables

Figures

◀

▶

◀

▶

Back

Close

Full Screen / Esc

Printer-friendly Version

Interactive Discussion

**Table 7.** Tritium and CFC concentrations in Takaka waters.

Date	Cl (mg/l)	Main Spring	Fish Spring	Balls bore
Tritium in TU				
27 May 1966	116	14.0±0.9		
29 July 1972	93	15.2±1.9		
20 March 1976	98	11.0±1.2		
26 Feb 1998	78	2.25±0.06		
16 March 1999		2.08±0.08		1.23±0.05
25 Aug 2000			1.96±0.06	
15 June 2005		1.42±0.04		
21 March 2006		1.53±0.05		
CFC-11 in pptv				
26 Feb 1998	78	206.1±4.7		109.3±4.7
21 Feb 2000		207.8±1.1		
25 Aug 2000			243.9±2.8	
3 Sep 2002			250.8±6.6	112.0±0.2
CFC-12 in pptv				
26 Feb 1998	78	453.6±6.5		264.5±1.0
21 Feb 2000		446.3±1.5		
25 Aug 2000			502.6±7.1	
3 Sep 2002		468.1±2.5	487.9±1.9	225.3±0.4



**Conceptual flow model for karst springs**

M. K. Stewart and  
J. T. Thomas

**Table 8.** Best-fit values of *b* and goodness-of-fit parameters for the 2-component model. The components are shallow system water (mean age 1.2 yr, DP 0.12) and deep system water (mean age 10.2 yr, DP 0.6).

Feature	Flow model		Tritium		CFC-11		CFC-12		Oxygen-18	
	<i>b</i>	sd	<i>b</i>	sd (TU)	<i>b</i>	sd (pptv)	<i>b</i>	sd (pptv)	<i>b</i>	sd (‰)
Main Spring	0.26	–	0.26	0.08	0.24	1.5	0.50	6.8	0.30	0.10
Fish Spring	0.75	–	0.67	0.00	0.81	2.6	0.70	7.2	0.75	0.14

Title Page

Abstract

Introduction

Conclusions

References

Tables

Figures

⏪

⏩

◀

▶

Back

Close

Full Screen / Esc

Printer-friendly Version

Interactive Discussion

## Conceptual flow model for karst springs

M. K. Stewart and  
J. T. Thomas

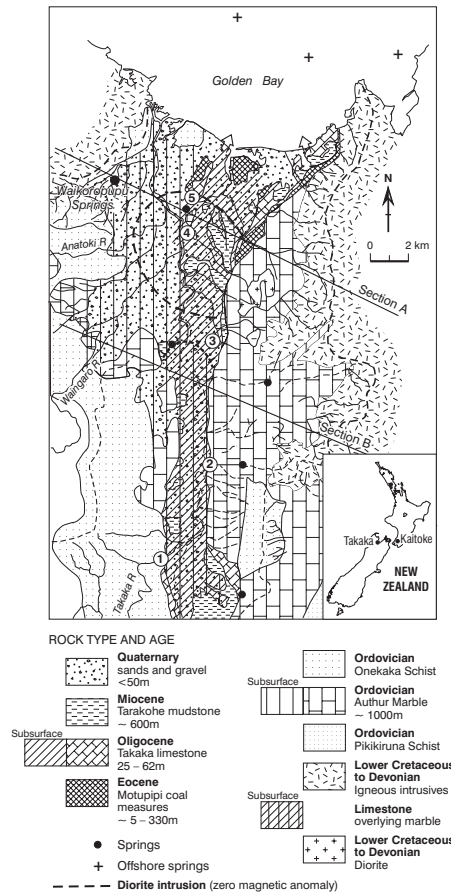


**Fig. 1.** Hydrogeological map of the Takaka Valley, NW Nelson, New Zealand (modified from Ford and Williams, 1989).

Title Page

Abstract

Introduction

Conclusions

References

Tables

Figures

⏪

⏩

◀

▶

Back

Close

Full Screen / Esc

Printer-friendly Version

Interactive Discussion

## Conceptual flow model for karst springs

M. K. Stewart and  
J. T. Thomas

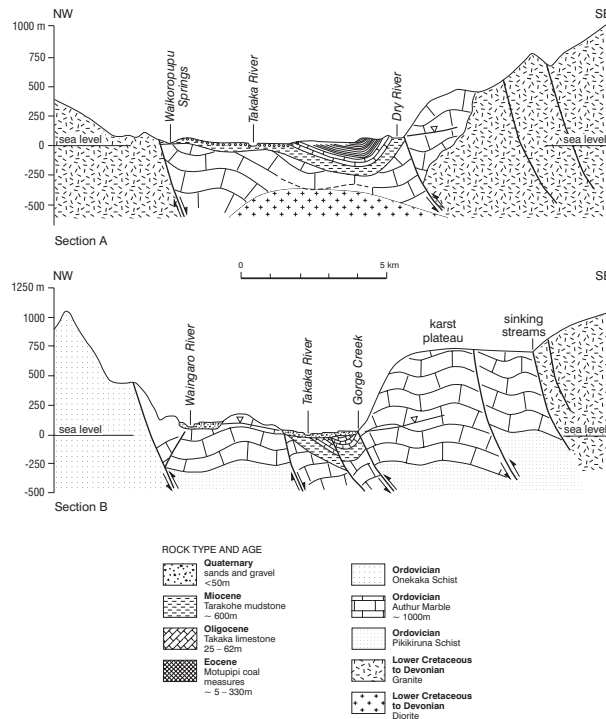


**Fig. 2.** Geological cross-sections of the Takaka Valley (modified from Ford and Williams, 1989).

Title Page

Abstract

Introduction

Conclusions

References

Tables

Figures

◀

▶

◀

▶

Back

Close

Full Screen / Esc

Printer-friendly Version

Interactive Discussion

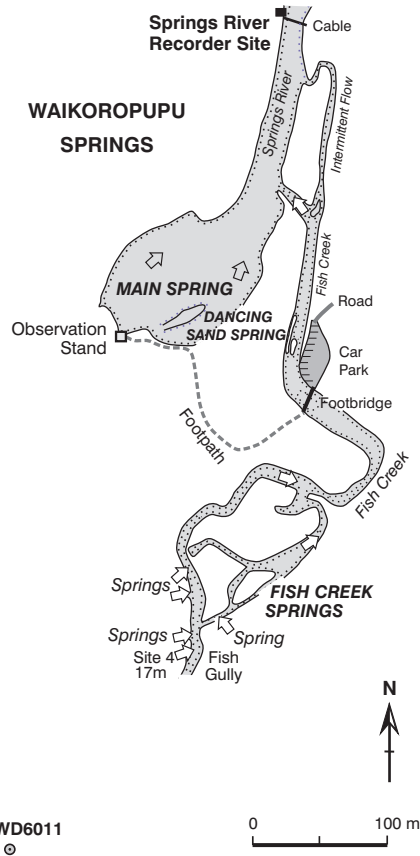


**Fig. 3.** Plan of the Waikoropupu Springs, showing the locations of the springs and Balls bore (WWD6011) (from Rapiere, 1975).

**Conceptual flow model for karst springs**

M. K. Stewart and J. T. Thomas

Title Page	
Abstract	Introduction
Conclusions	References
Tables	Figures
◀	▶
◀	▶
Back	Close
Full Screen / Esc	
Printer-friendly Version	
Interactive Discussion	

Conceptual flow model for karst springs

M. K. Stewart and J. T. Thomas

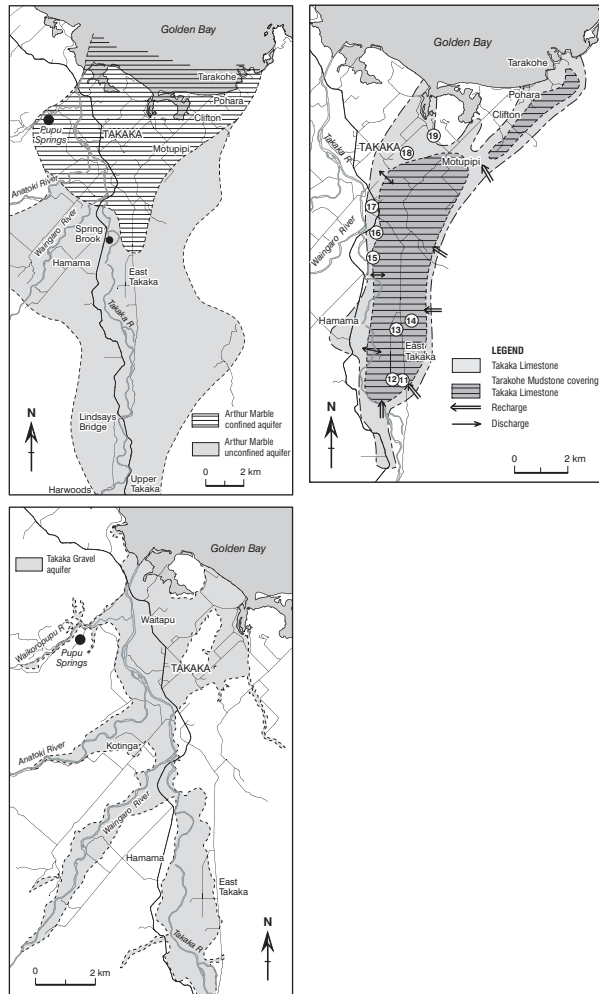


Fig. 4. (a) Arthur Marble Aquifer. (b) Takaka Limestone Aquifer (showing sample locations 11–19). (c) Takaka Gravel Aquifer. 1259

Title Page

Abstract

Introduction

Conclusions

References

Tables

Figures

⏪

⏩

◀

▶

Back

Close

Full Screen / Esc

Printer-friendly Version

Interactive Discussion

Conceptual flow model for karst springs

M. K. Stewart and J. T. Thomas

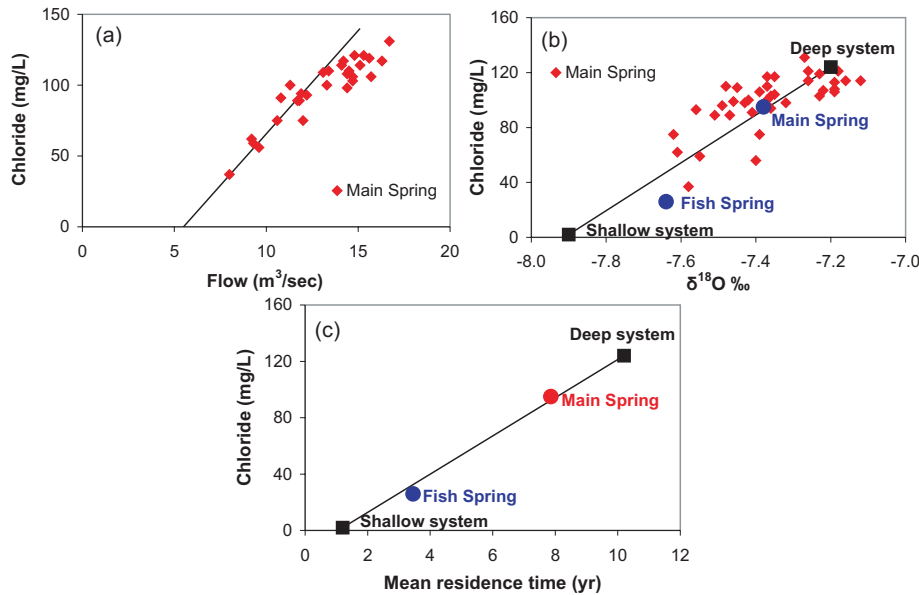


**Fig. 5.** (a) Springs River flow versus Main Spring chloride concentration. The line gives the approximate flow from the Main Spring alone. (b)  $\delta^{18}\text{O}$  versus chloride. (c) MRT versus chloride.

Title Page

Abstract

Introduction

Conclusions

References

Tables

Figures

⏪

⏩

◀

▶

Back

Close

Full Screen / Esc

Printer-friendly Version

Interactive Discussion

Conceptual flow model for karst springs

M. K. Stewart and J. T. Thomas

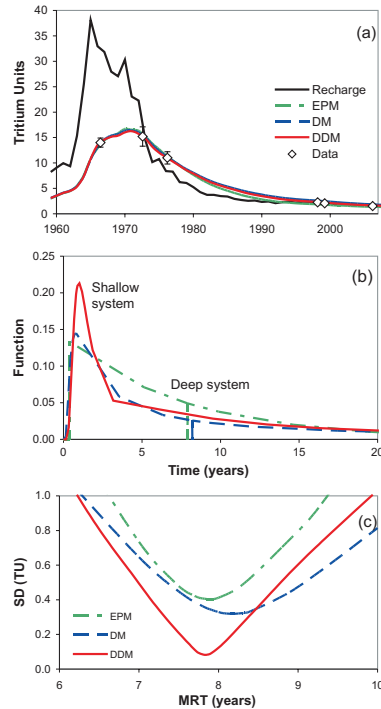


**Fig. 6.** Tritium results for the Main Spring. **(a)** Tritium concentrations in recharge, best-fit simulation models and spring water. **(b)** Distributions of residence times for best-fit simulation models. **(c)** Variation of the goodness-of-fit criterion with MRT.

Title Page

Abstract Introduction

Conclusions References

Tables Figures

⏪ ⏩

◀ ▶

Back Close

Full Screen / Esc

Printer-friendly Version

Interactive Discussion

Conceptual flow model for karst springs

M. K. Stewart and J. T. Thomas

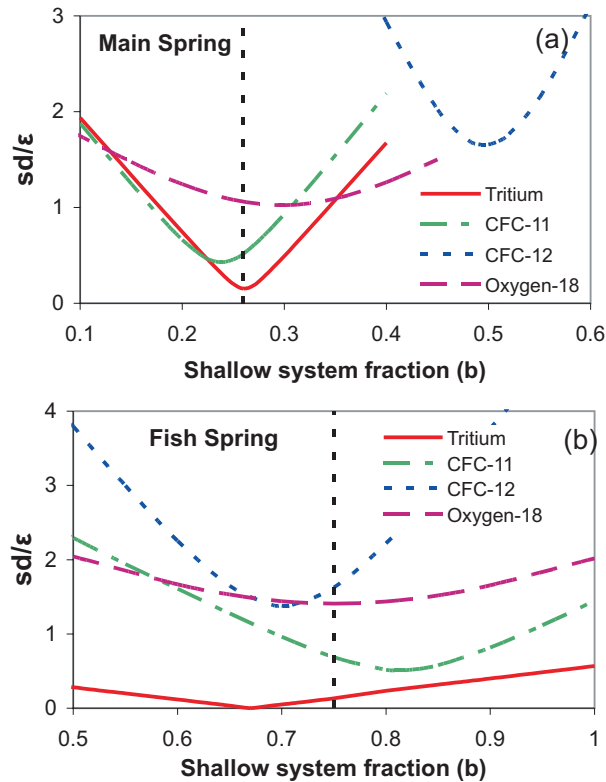


**Fig. 7.** Variation of the goodness-of-fit criterion with shallow system fraction ( $b$ ) for tritium, CFC-11, CFC-12 and oxygen-18 results. **(a)** Main Spring. **(b)** Fish Spring.

Title Page

Abstract

Introduction

Conclusions

References

Tables

Figures

◀

▶

◀

▶

Back

Close

Full Screen / Esc

Printer-friendly Version

Interactive Discussion



Conceptual flow model for karst springs

M. K. Stewart and J. T. Thomas

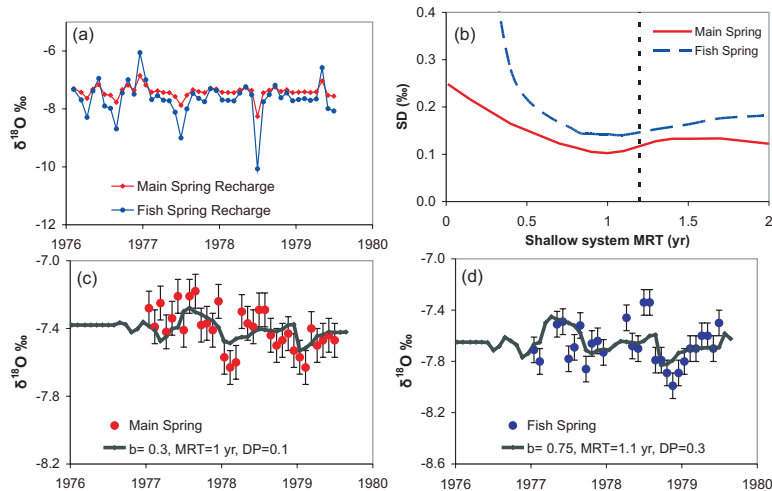


**Fig. 8.** Oxygen-18 results for the Main and Fish Springs. **(a)**  $\delta^{18}\text{O}$  variations in recharge to the springs. **(b)** Variation of the goodness-of-fit criterion with shallow system MRT. **(c)** Measurements and simulation for the Main Spring. **(d)** Measurements and simulation for Fish Spring.

Title Page

Abstract

Introduction

Conclusions

References

Tables

Figures

⏪

⏩

◀

▶

Back

Close

Full Screen / Esc

Printer-friendly Version

Interactive Discussion

Conceptual flow model for karst springs

M. K. Stewart and J. T. Thomas

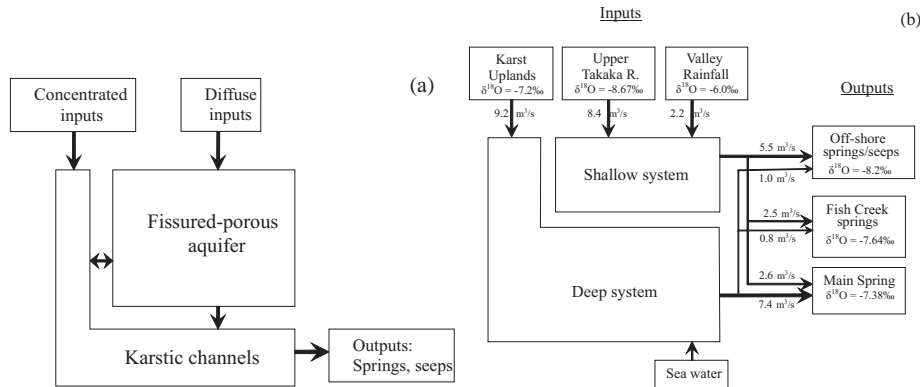


**Fig. 9.** Conceptual model of flow in the Arthur Marble Aquifer. **(a)** Schematic of flow in karst systems. **(b)** The relationship of inputs, flow systems and outputs in the AMA. The internal structure of the flow systems are as illustrated in (a). Average flows and  $\delta^{18}\text{O}$  values are shown.

Title Page	
Abstract	Introduction
Conclusions	References
Tables	Figures
◀	▶
◀	▶
Back	Close
Full Screen / Esc	
Printer-friendly Version	
Interactive Discussion	